

Boundary control of linearized Saint-Venant equations oscillating modes

Xavier Litrico and Vincent Fromion

Abstract—The Saint-Venant equations describe the dynamics of one dimensional open-channel flow. The paper investigates linearized Saint-Venant equations modes and their control. We show that it is possible to suppress the oscillating modes over all the canal pool by a well-designed boundary dynamic controller using only the water level measurement at the downstream end of the pool. This controller is infinite dimensional, and also not strictly proper, which makes it difficult to implement on a real canal. However, a static control of the oscillating modes can be performed with a well-designed hydraulic structure. We therefore study the specific case of a constant proportional controller on the oscillating modes and show that they can be asymptotically attenuated by using a controller that depends only on local flow characteristics. Experimental results on a laboratory canal pool show the effectiveness of the proposed control.

I. INTRODUCTION

The Saint-Venant equations describe the dynamics of open-channel hydraulic systems, e.g. rivers, irrigation or drainage canals, sewers, etc., assuming one dimensional flow. First stated in 1871, these nonlinear partial differential equations involving the discharge $Q(x, t)$ and the water depth $Y(x, t)$ along one space dimension x have been widely used by hydraulic engineers in their numerical models [4].

Many authors contributed on the control of open-channel hydraulic systems represented by Saint-Venant equations. The contributions range from classical SISO control methods such as Smith predictor [10] to LQG control [7] or H_∞ robust control [8]. Recent approaches tried to take into account the distributed feature of the system, either by using a semigroup approach [11], or by a Lyapunov approach [5].

To the best of our knowledge, no references deal with the problem of controlling the oscillating modes that appear on some types of canals, typically small canal pools. These modes are due to the interaction of upstream and downstream waves propagations which occur in subcritical flow (i.e. when the wave celerity is larger than the water velocity). Their amplitude can be very important for some hydraulic conditions [4]. This phenomenon also appears on the frequency response of linearized Saint-Venant equations with boundary conditions in terms of discharges [6] (see figure 1). The modes damping decreases when the discharge

decreases. They can lead to overspilling, which is highly undesirable for irrigation canals. Rather surprisingly, this problem has never been considered from a control point of view.

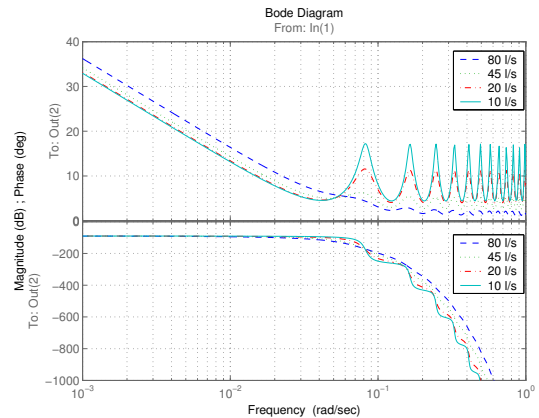


Fig. 1. Bode plot of the transfer function relating upstream discharge to downstream water elevation of a canal pool modelled with linearized Saint-Venant equations for different discharges and a constant downstream water elevation

The objective of the paper is to investigate linearized Saint-Venant equations modes and their control. We show that it is possible to suppress these oscillating modes over all the canal pool by a well-designed boundary dynamic controller using only the water level measurement at the downstream end of the pool. However, this controller is infinite dimensional, and also not strictly proper. This property makes it difficult to implement on a real canal, since the actuators have a finite bandwidth. We show that this difficulty can be bypassed in a real canal, which is usually controlled using hydraulic cross-structures such as gates or weirs. Such a hydraulic structure has an interesting feature: it structurally induces a local feedback between the discharge and the water level, whatever the frequency. That leads to investigate the effect of a proportional boundary controller on the oscillating modes. We obtain the gain value that achieves the best attenuation of oscillating modes over all the canal pool.

For practical applications, where any flow regime can be encountered, this study can only be done numerically. Nevertheless, it is possible to get a complete analysis in specific flow regimes (uniform flow), where closed-form solutions can be obtained. This study is of primary interest,

X. Litrico is with the Irrigation Research Unit, Cemagref, B.P. 5095, F-34033 Montpellier Cedex 1, France. xavier.litrico@cemagref.fr

V. Fromion is with the Laboratoire d'Analyse des Systèmes et Biométrie, INRA, 2 place Viala, 34060 Montpellier, France. fromion@ensam.inra.fr.

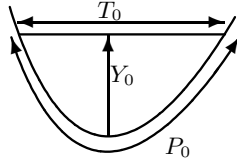


Fig. 2. Section of a canal

since we have recently shown that the properties of Saint-Venant equations are qualitatively the same whatever the flow regime [6].

These results are based on suitable simplifications of a mathematical model of open-channel flow dynamics. It is therefore important to validate the approach on a real canal. The experimental results obtained on a canal located in Portugal show the effectiveness of the proposed approach.

II. LINEARIZED SAINT-VENANT EQUATIONS

We present in this section the linearized Saint-Venant equations, used to obtain a transfer matrix representation of the system. A more detailed description is given in [6].

We consider in the paper a prismatic canal pool of length X with uniform geometry. As already stated in introduction, the Saint-Venant equations are hyperbolic nonlinear partial differential equations involving the average discharge $Q(x, t)$ and the water depth $Y(x, t)$ along one space dimension [2]. We consider small variations of discharge $q(x, t)$ and water depth $y(x, t)$ around stationary values $Q_0(x) = Q_0$ (m³/s) and $Y_0(x)$ (m) defined by

$$\frac{dY_0(x)}{dx} = \frac{S_b - S_{f0}(x)}{1 - F_0(x)^2} \quad (1)$$

where S_b is the bed slope, F_0 the Froude number $F_0 = \frac{V_0}{C_0}$ with V_0 the average velocity (m/s) and $C_0 = \sqrt{\frac{gA_0}{T_0}}$ the wave celerity (m/s), with T_0 the water surface top width (m), $A_0(x)$ the wetted area (m²) and g the gravitational acceleration (m/s²). Throughout the paper, the flow is assumed to be subcritical, i.e. $F_0 < 1$.

The friction slope S_{f0} is modelled with Manning-Strickler formula [2]:

$$S_{f0}(x) = \frac{Q_0^2 n^2}{A_0(x)^2 R_0(x)^{4/3}} \quad (2)$$

with n the roughness coefficient (sm^{-1/3}) and $R_0(x)$ the hydraulic radius (m), defined by $R_0 = A_0/P_0$ where P_0 is the wetted perimeter (m) (see figure 2).

Linearizing the Saint-Venant equations around these stationary values leads to (the dependance in x is omitted for readability, and we denote with small letters the deviations from stationary values):

$$T_0 \frac{\partial y}{\partial t} + \frac{\partial q}{\partial x} = 0 \quad (3)$$

$$\frac{\partial q}{\partial t} + 2V_0 \frac{\partial q}{\partial x} - \beta_0 q + (C_0^2 - V_0^2) T_0 \frac{\partial y}{\partial x} - \gamma_0 y = 0 \quad (4)$$

with $\beta_0 = -\frac{2g}{V_0} (S_b - \frac{dY_0}{dx})$, $\gamma_0 = V_0^2 \frac{dT_0}{dx} + gT_0 [(1 + \kappa_0)S_b - (1 + \kappa_0 - F_0^2)(\kappa_0 - 2)] \frac{dY_0}{dx}$ and $\kappa_0 = \frac{7}{3} - \frac{4A_0}{3T_0 P_0} \frac{dP_0}{dY}$.

The boundary conditions are the upstream and downstream discharges $q(0, t)$ and $q(X, t)$.

When the water depth is constant along the channel, the left side of equation (1) is equal to zero and then, given $Q_0(x) = Q_0$, the equilibrium solution Y_0 can be deduced by solving the following algebraic equation:

$$S_f(Q_0, Y_0) = S_b \quad (5)$$

Analytical results with closed-form solutions can be obtained in that case, called ‘‘uniform flow’’.

We illustrate the paper on an experimental canal of the University of Évora, located in Portugal. The experimental canal is a trapezoidal and lined canal, with a general cross section of bottom width 0.15 m, sides slope 1:0.15 (V:H) and depth 0.90 m. The considered pool is 75 m long and the average longitudinal bottom slope is about 1.5×10^{-3} . The Manning friction coefficient is equal to 0.016 sm^{-1/3}.

III. ANALYTICAL RESULTS IN UNIFORM FLOW

We develop here the complete results obtained in the uniform case. First the Saint-Venant open-loop transfer matrix is characterized, then the optimal dynamic controller for the oscillating modes is obtained. The special case of a proportional static controller is then considered.

A. Open-loop transfer matrix characterization

1) *Saint-Venant transfer matrix*: The Saint-Venant open-loop transfer matrix can be obtained by applying Laplace transform to the linear partial differential equations (3–4), and solving the resulting system of Ordinary Differential equations in the variable x , parameterized by the Laplace variable s [6].

On this basis, the Saint-Venant transfer matrix relating the water depth $y(x, s)$ and the discharge $q(x, s)$ at any point in the canal to the upstream and downstream discharges is given by [3], [9]:

$$y(x, s) = g_{11}(x, X, s)q(0, s) + g_{12}(x, X, s)q(X, s) \quad (6)$$

$$q(x, s) = g_{21}(x, X, s)q(0, s) + g_{22}(x, X, s)q(X, s) \quad (7)$$

with

$$g_{11}(x, X, s) = \frac{\lambda_2 e^{\lambda_2 x + \lambda_1 X} - \lambda_1 e^{\lambda_1 x + \lambda_2 X}}{T_0 s (e^{\lambda_2 X} - e^{\lambda_1 X})} \quad (8)$$

$$g_{12}(x, X, s) = \frac{\lambda_1 e^{\lambda_1 x} - \lambda_2 e^{\lambda_2 x}}{T_0 s (e^{\lambda_2 X} - e^{\lambda_1 X})} \quad (9)$$

$$g_{21}(x, X, s) = \frac{e^{\lambda_1 x + \lambda_2 X} - e^{\lambda_2 x + \lambda_1 X}}{e^{\lambda_2 X} - e^{\lambda_1 X}} \quad (10)$$

$$g_{22}(x, X, s) = \frac{e^{\lambda_2 x} - e^{\lambda_1 x}}{e^{\lambda_2 X} - e^{\lambda_1 X}} \quad (11)$$

and the eigenvalues are given by:

$$\lambda_{1,2}(s) = \frac{1}{C_0(1 - F_0^2)} \left[F_0 s + \frac{gS_b(1 + \kappa_0)}{2C_0} \mp \sqrt{\delta(s)} \right] \quad (12)$$

with $\delta(s) = s^2 + \frac{gS_b(2 + (\kappa_0 - 1)F_0^2)}{V_0} s + \frac{g^2 S_b^2 (1 + \kappa_0)^2}{4C_0^2}$.

$$G_{k_u}^{(1)}(x, X, s) = \frac{\lambda_2 e^{\lambda_2 x + \lambda_1 X} - \lambda_1 e^{\lambda_1 x + \lambda_2 X} + k_u(s) \frac{\lambda_1 \lambda_2}{T_0 s} (e^{\lambda_2 x + \lambda_1 X} - e^{\lambda_1 x + \lambda_2 X})}{T_0 s (e^{\lambda_2 X} - e^{\lambda_1 X}) + k_u(s) (\lambda_2 e^{\lambda_2 X} - \lambda_1 e^{\lambda_1 X})} \quad (13)$$

$$G_{k_u}^{(2)}(x, X, s) = \frac{T_0 s (e^{\lambda_1 x + \lambda_2 X} - e^{\lambda_2 x + \lambda_1 X}) + k_u(s) (\lambda_2 e^{\lambda_1 x + \lambda_2 X} - \lambda_1 e^{\lambda_2 x + \lambda_1 X})}{T_0 s (e^{\lambda_2 X} - e^{\lambda_1 X}) + k_u(s) (\lambda_2 e^{\lambda_2 X} - \lambda_1 e^{\lambda_1 X})} \quad (14)$$

2) *Poles of Saint-Venant transfer matrix:* The open-loop poles of Saint-Venant transfer matrix are obtained as the solutions of equation $T_0 s (e^{\lambda_2(s)X} - e^{\lambda_1(s)X}) = 0$. There is a pole in zero (the canal pool acts as an integrator) and the other poles verify the following equation:

$$s^2 + \frac{2gS_b}{V_0} \left(1 + \frac{\kappa_0 - 1}{2} F_0^2\right) s + \frac{g^2(1 + \kappa_0)^2 S_b^2}{4C_0^2} + \frac{k^2 \pi^2 C_0^2 (1 - F_0^2)^2}{X^2} = 0$$

with $k \in \mathbb{N}^*$ (the pole obtained for $k = 0$ simplifies with a zero).

When $S_b \neq 0$, the poles p_k are then given by:

$$p_k = \frac{gS_b}{V_0} \left[-1 - \frac{\kappa_0 - 1}{2} F_0^2 \pm (1 - F_0^2) \sqrt{\Delta(k)} \right] \quad (15)$$

$$\text{with } \Delta(k) = \frac{1 - \frac{(\kappa_0 - 1)^2}{4} F_0^2}{1 - F_0^2} - \frac{k^2 \pi^2 C_0^2 V_0^2}{g^2 S_b^2 X^2}.$$

Let $k_m \in \mathbb{N}$ be the greatest integer such that $\Delta(k_m) \geq 0$; then the poles obtained for $0 < k \leq k_m$ are negative real, and those obtained for $k > k_m$ are complex conjugate, with a constant real part (they are located on a vertical line in the left half plane). Moreover, for $k \gg 1$ the poles can be approximated by:

$$p_k \approx -\frac{(\alpha_1 + \alpha_2)X}{\tau_1 + \tau_2} \pm \frac{2jk\pi}{\tau_1 + \tau_2} \quad (16)$$

with $\alpha_1 = \frac{T_0 S_b (2 - (\kappa_0 - 1) F_0)}{2 A_0 F_0 (1 + F_0)}$, $\alpha_2 = \frac{T_0 S_b (2 + (\kappa_0 - 1) F_0)}{2 A_0 F_0 (1 - F_0)}$ and $\tau_1 = \frac{X}{C_0 + V_0}$ the delay for downstream propagation, $\tau_2 = \frac{X}{C_0 - V_0}$, the delay for upstream propagation.

This approximation allows to recover the classical approximation for oscillating modes, corresponding to the interaction of two gravity waves, one travelling downstream at speed $V_0 + C_0$ with attenuation factor α_1 , and one travelling upstream at speed $C_0 - V_0$ with attenuation factor α_2 . Indeed, with such an approximation, the transfer function denominator is given by:

$$D(s) = 1 - e^{-(\alpha_1 + \alpha_2)X - (\tau_1 + \tau_2)s}$$

whose roots coincide with the poles approximation (16).

Characterizing oscillating canal pools: Equation (15) enables to characterize two types of canal, based on a non dimensional variable $\chi = \frac{X S_b T_0}{A_0}$ classically considered by hydraulic engineers [1]. To this purpose, let us introduce the limit value given by:

$$\chi_c = \pi F_0 \sqrt{\frac{1 - F_0^2}{1 - \frac{(\kappa_0 - 1)^2}{4} F_0^2}} \quad (17)$$

which corresponds to $\Delta(1) = 0$, and thus the minimum value such that the first pole remains real. Then, if $\chi \ll \chi_c$, the predominant hydraulic behavior is mainly linked to surface waves interaction and if $\chi \gg \chi_c$, the predominant behavior is linked to the mass transfer.

We focus in the paper on the canal pools with a dominant oscillating behavior, i.e. corresponding to $\chi < \chi_c$.

B. Optimal mode dampening: dynamic controller

1) *Closed-loop transfer matrix:* Let the system be controlled with a local upstream linear boundary controller relating the water level and the discharge at X , the downstream end of the pool:

$$q(X, s) = k_u(s) y(X, s) \quad (18)$$

The closed-loop system is then given by:

$$\begin{pmatrix} y(x, s) \\ q(x, s) \end{pmatrix} = \begin{pmatrix} G_{k_u}^{(1)}(x, X, s) \\ G_{k_u}^{(2)}(x, X, s) \end{pmatrix} q(0, s) \quad (19)$$

with $G_{k_u}^{(1)}(x, X, s)$ and $G_{k_u}^{(2)}(x, X, s)$ respectively given by equations (13) and (14) displayed on top of the page.

Transfer functions $G_{k_u}^{(1)}(x, X, s)$ and $G_{k_u}^{(2)}(x, X, s)$ describe the frequency response of the water level and the discharge in any point x as a function of upstream discharge with a local controller $k_u(s)$ at the downstream end of the canal pool. Such a local controller can be used to control the modes of the Saint-Venant equation.

2) *Dynamic boundary control of oscillating modes:* We show in this section that it is possible to remove oscillating modes over all the canal pool by using a dynamic boundary controller.

Theorem 1: With a downstream boundary control defined by

$$k_u^*(s) = -\frac{T_0 s}{\lambda_1(s)} \quad (20)$$

the canal pool at uniform flow represented by the transfer matrix (6–7) has no oscillating modes.

Proof: The oscillating poles of the closed-loop system are solutions of the equation:

$$e^{(\lambda_2(s) - \lambda_1(s))X} - \frac{T_0 s + k_u(s) \lambda_1(s)}{T_0 s + k_u(s) \lambda_2(s)} = 0 \quad (21)$$

With the controller $k_u^*(s)$ given by equation (20), we get:

$$e^{(\lambda_2(s) - \lambda_1(s))X} = 0 \quad (22)$$

which has no solution and thus the system has no oscillating modes. ■

Let us note that for any $x \in [0, X]$ the transfer functions $G_{k_u^*}^{(1)}$ and $G_{k_u^*}^{(2)}$ are given by:

$$G_{k_u^*}^{(1)}(x, X, s) = -\frac{\lambda_1(s)}{T_0 s} e^{\lambda_1(s)x}$$

$$G_{k_u^*}^{(2)}(x, X, s) = e^{\lambda_1(s)x}$$

and thus the only the downstream propagating waves remain. The canal is behaving as if it was semi-infinite, i.e. the waves propagating downstream do not reflect on the

downstream boundary and the oscillating modes then disappear. This is similar to the classical concept of “impedance matching” for electrical networks.

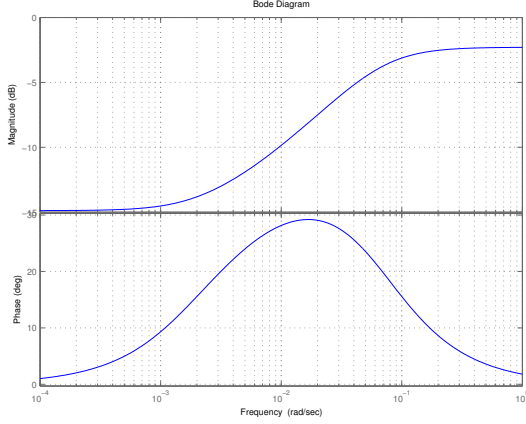


Fig. 3. Bode plot of $k_u^*(s)$ for the experimental canal of the University of Évora, discharge $Q_0 = 0.06 \text{ m}^3/\text{s}$, water depth $Y_0 = 0.56 \text{ m}$.

The Bode diagram of $k_u^*(s)$ is depicted in figure 3 for a canal pool. This stable, infinite-dimensional controller strongly looks like a lead-lag filter. It is not strictly proper, since it has a constant gain in high frequencies, given by:

$$\lim_{\omega \rightarrow \infty} k_u^*(j\omega) = T_0(V_0 + C_0) \quad (23)$$

Because it is not strictly proper, such a controller seems difficult to implement on a real canal. This is true when the control input is a discharge, since in this case, the actuator bandwidth is necessarily limited. However, a constant gain in high frequency can be implemented by using the structural property of hydraulic structures such as gates or weirs.

A hydraulic cross-structure is usually described by a static nonlinear relation (obtained from Bernoulli’s law) $Q = f(Y, W)$, where Q is the absolute discharge, Y the water depth and W the gate opening or weir elevation. When considering small variations around stationary values, one gets the linearized equation $q = k_1 y + k_2 w$ with $k_1 = \frac{df}{dY}$ and $k_2 = \frac{df}{dW}$. The gate opening w being typically controlled by an electrical actuator, the bandwidth limitation applies and the optimal controller cannot be implemented by “dynamic” feedback through k_2 . It is thus only possible to use the local static feedback k_1 that directly links the water level y to the discharge q to achieve a high frequency control politics.

Moreover, we observe that at a frequency close to 10^{-1} rad/s (corresponding to the first oscillating mode), the amplitude of the lead-lag filter has already reached its asymptotic value (see figure 3), which justifies the use of a proportional controller.

We will now study the effect of different values of k_u (that can be obtained with different gate characteristics) on the oscillating modes by doing a root locus.

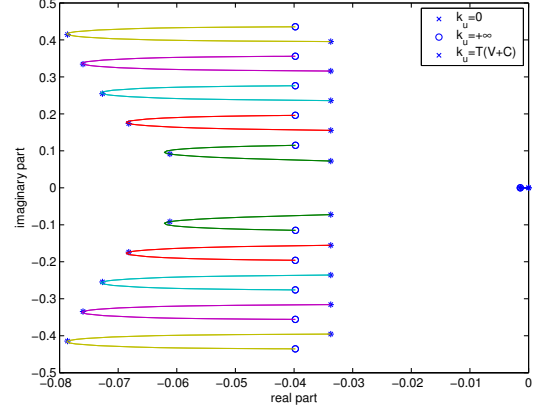


Fig. 4. Roots locus for the Évora canal, discharge $Q_0 = 0.06 \text{ m}^3/\text{s}$, water depth $Y_0 = 0.56 \text{ m}$: poles (+) obtained for $k_u = 0$, zeros (o) obtained for $k_u = +\infty$, and closed-loop poles location (*) for $k_u^* = T_0(V_0 + C_0)$

C. Static boundary proportional controller

The closed-loop system poles for a local upstream proportional controller of gain $k_u \in \mathbb{R}^+$ are given by the solutions of equation:

$$\psi(s) := e^{(\lambda_2(s) - \lambda_1(s))X} - \frac{T_0 s + k_u \lambda_1(s)}{T_0 s + k_u \lambda_2(s)} = 0 \quad (24)$$

In general, there is no closed-form solution of equation (24). However, it is possible to study the asymptotic root locus for $|s| \gg 1$. We have the following

Proposition 1: When $|s| \gg 1$, the solutions of equation (24) tend asymptotically towards

$$\tilde{p}_k = -\frac{(\alpha_1 + \alpha_2)X}{\tau_1 + \tau_2} - \frac{1}{\tau_1 + \tau_2} \log \left(\frac{T_0 X + k_u \tau_2}{T_0 X - k_u \tau_1} \right) \pm \frac{2jk\pi}{\tau_1 + \tau_2} \quad (25)$$

The proof is omitted for lack of space.

We recover the poles approximation of (16) when $k_u = 0$. When k_u increases, the poles real part diminishes towards $-\infty$ for $k_u < T_0(C_0 + V_0)$. Then, it increases when $k_u > T_0(C_0 + V_0)$, to finally tend towards $-\frac{(\alpha_1 + \alpha_2)X}{\tau_1 + \tau_2} - \frac{1}{\tau_1 + \tau_2} \log \left(\frac{\tau_2}{\tau_1} \right)$ when $k_u \rightarrow \infty$.

This also explains why poles and zeros are “intertwined” or alternate along the imaginary axis. Zeros are obtained for $k_u = +\infty$ and have a real part smaller than the one of the open-loop poles (because $\tau_1 < \tau_2$); their imaginary part is given by $\pm(2k+1)\pi/(\tau_1 + \tau_2)$, because the complex logarithm verifies $\log(-1) = \pm j\pi$. This explains why the poles and zeros alternate along the imaginary axis.

Figure 4 shows the root locus for the Évora canal, used in the experimental section.

Figures 5, 6 and 7 represent the Bode diagram of the local upstream controlled canal along the longitudinal abscissa x , with different gains: $k_u = 0$ in figure 5, $k_u = +\infty$ in figure 6, and $k_u^* = T_0(V_0 + C_0)$ in figure 7. It is clear that a constant controller k_u^* dramatically dampens the oscillation modes over all the canal pool. Indeed, a constant controller leads to a very close performance to the one obtained with a dynamic controller $k_u(s)$.

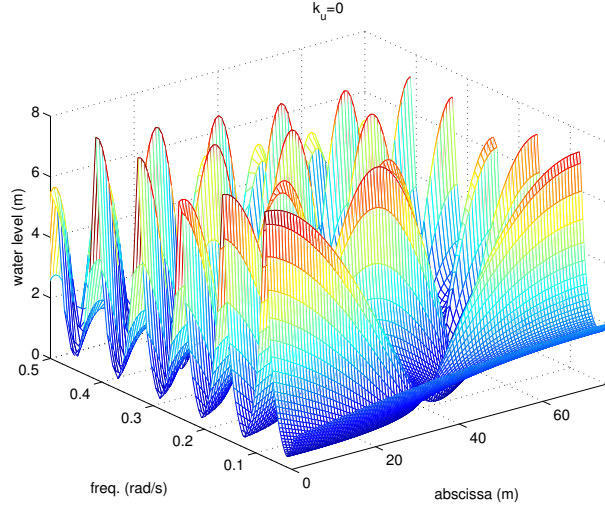


Fig. 5. Spatial Bode diagram of the canal in open-loop ($k_u = 0$)

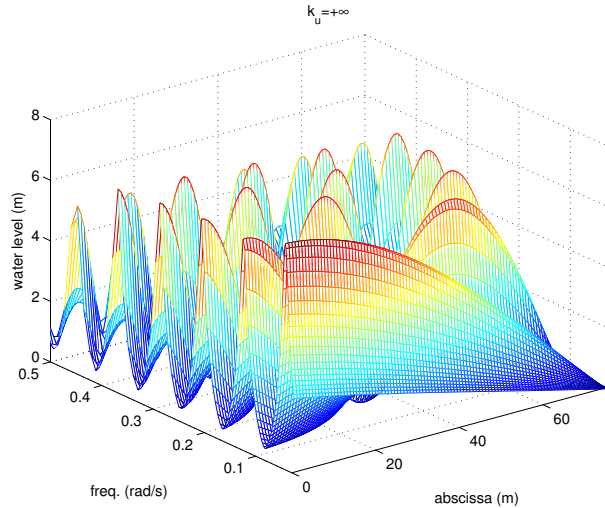


Fig. 6. Spatial Bode diagram of the local upstream controlled canal with $k_u = +\infty$

With such a local upstream proportional controller, the water level oscillations can be damped from 25% to 170% according to the abscissa and up to 80% for the discharge oscillations.

D. Local downstream control of oscillating modes

Similar results can be obtained for a local downstream controller $q(0, s) = k_d(s)y(0, s)$. In that case, for the optimal controller, the waves travelling upstream are not reflected on the upstream boundary. The optimal controller $k_d^*(s)$ is given by:

$$k_d^*(s) = -\frac{T_0 s}{\lambda_2(s)}$$

The corresponding static gain in high frequencies is given by:

$$\lim_{\omega \rightarrow \infty} k_d^*(j\omega) = T_0(V_0 - C_0) \quad (26)$$

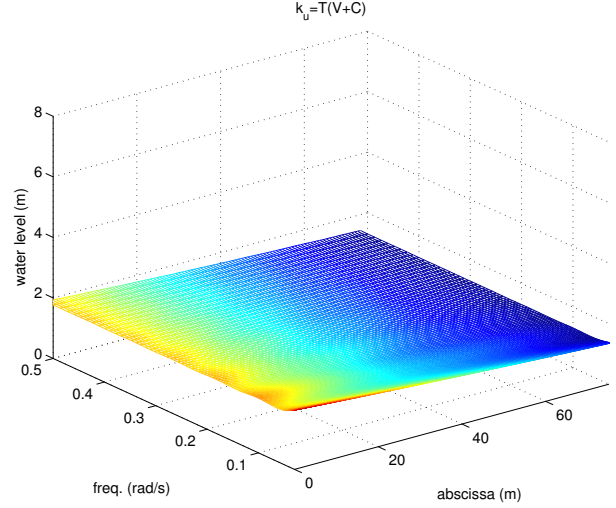


Fig. 7. Spatial Bode diagram of the local upstream controlled canal with $k_u^* = T_0(C_0 + V_0)$

IV. EXTENSION TO NON-UNIFORM FLOW

For non-uniform flow conditions, there are no more analytical results concerning Saint-Venant equations. The Saint-Venant transfer matrix is obtained by solving the ordinary differential equation:

$$\frac{d}{dx} \begin{pmatrix} q(x, s) \\ y(x, s) \end{pmatrix} = \mathcal{A}_s(x) \begin{pmatrix} q(x, s) \\ y(x, s) \end{pmatrix} \quad (27)$$

with $\mathcal{A}_s(x) = \begin{pmatrix} 0 & -T_0(x)s \\ \frac{-s+\beta_0(x)}{T_0(x)(C_0(x)^2-V_0(x)^2)} & \frac{2V_0(x)T_0(x)s+\gamma_0(x)}{T_0(x)(C_0(x)^2-V_0(x)^2)} \end{pmatrix}$, and the solution has to be computed numerically (see [6] for computational aspects).

However, the asymptotic behavior in high frequencies can be shown to be similar as in uniform flow, i.e. for $|s| \gg 1$, the controller $k_u^*(s)$ tends towards a constant gain, equal to $T_0(X)(C_0(X) + V_0(X))$.

Therefore, for high frequencies, the “optimal” controller k_u^* is only determined by the local characteristics of the flow. The corresponding gain leads to similar graphs as figures 5, 6 and 7 in non uniform flow.

We have therefore shown that it is possible to attenuate the resonant modes over all the canal pool by using a well-designed proportional boundary control. This controller uses only boundary water levels measurements. In this control problem, the overall performance is not only linked to the behavior at the boundary of the canal pool, since the problem is a distributed one. This is usually hidden in the classical input-output view of the problem. A remarkable fact is that a simple proportional boundary controller enables to ensure good performance *over all the canal pool*. This result will be tested experimentally in the following section.

V. APPLICATION

For the Évora canal, which is an experimental canal, we could use an very rapid actuator (a motorized valve)

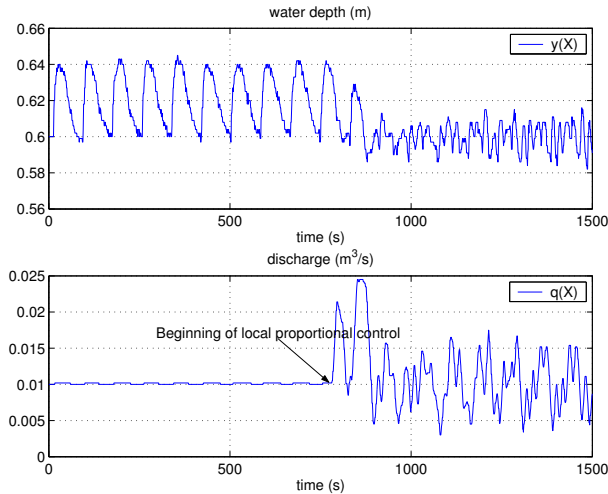


Fig. 8. Water level $y(X)$ and outlet discharge without and with the local proportional controller k_u^*

that enabled to bypass the bandwidth limitation problem. The controller was tested for the first oscillating mode, in reaction to an upstream sinusoidal input at the resonant frequency.

The canal inlet is equipped with a motorized flow control valve, that delivers a discharge u_1 . The canal pool is excited with a sinusoidal input discharge $u_1 = 0.01 + 0.005 \sin \omega t$, with $\omega = 0.082$ rad/s, corresponding to the first oscillating mode frequency. There is an offtake p at the downstream end of the pool of the orifice type with additional external pipe, equipped with an electromagnetic flowmeter and a motorized butterfly valve. Five water level sensors are installed within offline stilling wells distributed along the canal pool. Only the sensor located at the downstream end is used by the controller. The other sensors are used for illustration purposes. The controller is implemented on the offtake p , which can react quickly. No control is performed until $t = 1250$ s (i.e. the outlet discharge is imposed to a constant value). Then, the controller is put on (see figure 8). The water level oscillations are dramatically reduced, and this is also the case along the whole canal pool (see figure 9).

VI. CONCLUSION

The paper provides a detailed study of the oscillating modes of linearized Saint-Venant equations. We show that a local boundary dynamic controller can exactly dampen the modes. A proportional local control can also be efficient to dampen the modes. A root locus technique is used to characterize the poles behavior, with an asymptotic study for high frequencies. Experimental results on a real canal show the effectiveness of the control method.

This result sheds a new light on the usefulness of gates in open-channels: from a control point of view, they were classically analyzed as elements inducing a coupling between canal pools. The system then becomes multivariable, which

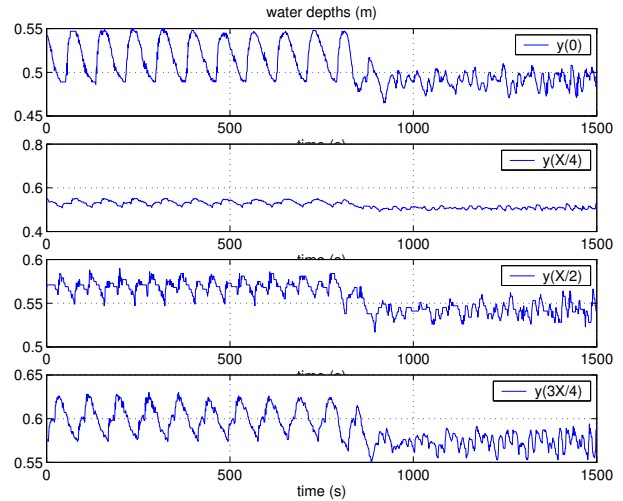


Fig. 9. Water levels along the canal without and with the local proportional controller k_u^*

makes difficult the design of decentralized controllers. We show here that the gates also have a great interest: they stabilize the canal pool and dampen the oscillating modes, which were considered as difficult to control directly.

VII. ACKNOWLEDGMENTS

The authors gratefully acknowledge the financial help of Cemagref and INRA through the collaborative program ASS AQUAE n° 2.

The experimental part was supported by the French Embassy in Portugal and GRICES (Gabinete de Relações Internacionais da Ciência e do Ensino Superior) of Portugal, through the collaboration project n° 547-B4. We thank Prof. Manuel Rijo from the University of Évora for his help and hospitality during our stays in Portugal.

REFERENCES

- [1] J.P. Baume, J. Sau, and P.-O. Malaterre. Modeling of irrigation channel dynamics for controller design. In *Conf. on Systems, Man and Cybernetics, SMC'98*, pages 3856–3861, San Diego, 1998.
- [2] V.T. Chow. *Open-channel Hydraulics*. McGraw-Hill Book Company, New York, 1988. 680 p.
- [3] G. Corriga, F. Patta, S. Sanna, and G. Usai. A mathematical model for open-channel networks. *Appl. Math. Modelling*, 3:51–54, 1979.
- [4] J.A. Cunge, F.M. Holly, and A. Verwey. *Practical aspects of computational river hydraulics*. Pitman Advanced Publishing Program, 1980.
- [5] J. de Halleux, C. Prieur, J.-M. Coron, B. d'Andéa Novel, and G. Bastin. Boundary feedback control in networks of open-channels. *Automatica*, 39:1365–1376, 2003.
- [6] X. Litrico and V. Fromion. Frequency modeling of open channel flow. *J. of Hydraulic Engineering*, 2004. in press.
- [7] P.-O. Malaterre. *Modélisation, analyse et commande optimale LQR d'un canal d'irrigation*. Ph.D. thesis, ENGREF - Cemagref, 1994.
- [8] P. Pognant-Gros, V. Fromion, and J.P. Baume. Canal controller design: a multivariable approach using H_∞ . In *European Control Conference*, pages 3398–3403, Porto, 2001.
- [9] J. Schuurmans. *Control of water levels in open-channels*. Ph.D. thesis, ISBN 90-9010995-1, Delft University of Technology, 1997.
- [10] M.J. Shand. *Automatic downstream control systems for irrigation canals*. Ph.D. thesis, University of California, Berkeley, 1971.
- [11] C.Z. Xu and G. Sallet. Proportional and integral regulation of irrigation canal systems governed by the St Venant equation. In *14th Triennial World Congress, IFAC 99*, volume E-2c-10-2, pages 147–152, Beijing, China, 1999.